Intracellular signal propagation in a two-dimensional autocatalytic reaction model

F. Castiglione,* M. Bernaschi,† and S. Succi‡
IAC "Mauro Picone" (CNR), Viale del Policlinico 137, 00161 Rome, Italy

R. Heinrich§
Department of Theoretical Biophysics, Humboldt University, Invalidenstrasse 42, D-10115 Berlin, Germany

M. W. Kirschner‖
Department of Cell Biology, Harvard Medical School, 240 Longwood Avenue, Boston, Massachusetts 02115
(Received 14 December 2001; published 19 September 2002)

We study a simple reaction scheme in a two-dimensional lattice of particles or molecules with a refractory state. We analyze the dynamics of the propagating front as a function of physical-chemical properties of the host medium. The anisotropy of the medium significantly affects the smoothness of the wave front. Similarly, if particles or molecules may diffuse slowly to neighboring sites, then the front wave is more likely to be irregular. Both situations affect the ability of the whole system to relax to the original state, which is a required feature in the biological cells. Attempts to map this simple reaction scheme to reactions involved in the intracellular pathways suggest that, in some cases, signal transduction might take both connotation of a random walk and a propagating wave, depending on the local density of the medium. In particular, a sufficient condition for the appearance of waves in high-density regions of the media, is the existence of at least one autocatalytic reaction in the chain of reactions characterizing the pathway.

DOI: 10.1103/PhysRevE.66.031905 PACS number(s): 87.16.Ac, 89.90.+n

I. INTRODUCTION

In the recent years, considerable effort has been directed toward the development of computer models aimed at simulating the intracellular complexity of a large number of molecular interactions [1–3]. In particular, intracellular signaling (or *signal transduction* [4]), namely the mechanism by which extracellular signals are converted into cellular responses, has attracted considerable attention. Molecules involved in the pathways are usually multifunctional in that they are generally involved in more than a single pathway. Well-known examples are the MAP (mitogen-activated protein) kinase pathways [5] and the Wnt (wingless network, network of gene interaction) pathways [6,7]. Understanding the role of each single molecule in multisignal pathways is a difficult task for experimental investigation [4,6,8,9], whence the motivation for computer simulations.

In this paper, we present a computer model focused on the particular problem of signal propagation.

A. Wave versus random diffusion translocation

The process of translocating to the nucleus is still only partially understood in physical terms. Experiments using fluorescent techniques show that in some cases the signal-carrying molecules diffuse randomly all the way down to the nucleus. This simple mechanism of translocation is supported by the fact that the diffusivity of a generic protein in the cytosol is quite high. Nevertheless, a random diffusion translocation cannot explain the whole story because it entails delays much larger than those observed experimentally when the distance to be covered is large. For instance, in eggs with a diameter of about 1 mm, a signal traveling from the cell membrane to the nucleus would take days. An alternative to this scenario is that the signal, represented by the ''active'' state of certain molecules, is transferred among neighboring molecules by means of chemical reactions.

Indeed, chemical waves are found in many aspects of cell behavior. For example, calcium waves [10], aggregation of Dictyostelium amoebas [11,12], membrane polarization in nerve axons, and cytosolic calcium waves in Zebrafish eggs development [13]. Simply speaking, wave propagation is known to be more efficient (faster) than random diffusion in propagating a signal at speed u over a distance l, whenever $ul/D>1$, D being the molecular diffusivity. Diffusion is the ''preferential direction'' of the wave front.

In the following, we investigate such a hypothesis and perform computer simulations of different scenarios aimed at reproducing realistic settings. One of such scenario considers a nonhomogeneous medium. Another scenario accounts for the diffusion of the molecules involved in the propagation of the signal.

The main result of this work is that signal propagation may well be the occurrence of both random diffusion and wave propagation. Understanding the interplay of these two different physical phenomena is relevant since it determines the time delays observed in cell coordination, metabolic responses, behavioral activation, and/or switching through intracellular in general.

In the last section, we propose two different set of reactions which may be involved in pathways leaving space to

*On leave from the Department of Cell Biology, Harvard Medical School, Boston, MA; email address: filippo@iac.rm.cnr.it
†Email address: massimo@iac.rm.cnr.it
‡Email address: succi@iac.rm.cnr.it
§Email address: reinhart.heinrich@biologie.hu-berlin.de
‖Email address: marc.kirschner@hms.harvard.edu

further refinements and, hopefully, to experimental investigation.

II. CHEMICAL WAVES IN REACTION SYSTEMS

Autocatalytic reaction systems and their front propagation in various dimensions have been extensively studied [14]. The simplest and classical case of nonlinear reaction-diffusion equation has been originally proposed by Fisher as a deterministic version of a stochastic model for the spatial spread of a favored gene in a population [15] and further explored by Kolmogoroff *et al.* [16]. One of the most famous applications of the aforementioned reaction-diffusion system is the so-called Belousov-Zhabotinskii (BZ) reaction [17–19], which is widely regarded as a prototypical example of oscillating chemical reactions.

In Ref. [20] an excitable medium is modeled by means of a CA (cellular automata) in which each site is characterized by internal state variables. To reflect the typical phase portrait of excitable media, two-state variables are employed: an excitation variable and a recovery variable. It is known that models of this sort exhibit all the generic features of waves in an excitable media [21]. A very simple discrete model is the *burnt bridge model* (BBM) [22].

The BBM is defined on a one-dimensional lattice. Nodes of the lattice represent links, some of which are called bridges. A random walker starts on the left side of the lattice and proceeds crossing the links at each time step. Once the walker crosses a bridge from left to right, the bridge is burnt with a certain probability. Attempts to cross a bridge from right to left also burn the bridge with the same probability. It is clear that as long as the walker proceeds along its walk, the bridges at his left are likely to be burnt, so that the walk is biased to the right. The velocity of the front identified with the walker depends on the probability at which the bridges are burnt. Initially all but one molecule are in the inactive state *I*, while the active molecule *A* is placed on the left of the linear lattice. The random path is given by the activation of the neighboring molecules. This model is equivalent to the discrete version of the reaction $A+I\rightarrow 2A$. This is obtained by replacing the walker by an active molecule and setting the probability to burn the bridge to 1.

The BBM and the Belousov-Zhabotinskii reactions as well as many other models of this sort are based on a simple scheme. In a discrete system, one has three-state nodes: resting or inactive (I), active (A), and exhausted or refractory (R). A certain number of active nodes can activate a resting node, which thereupon enters into the exhausted state for several generations. Once the recovery time has elapsed, an inactive node rests until activated anew. This simple recipe produces wave patterns very similar to those observed in biological systems.

We have developed a cellular automata model to study the spatial features of the propagation of a signal much like the automaton discussed in Refs. [21,22], whose continuous study has been formulated in two dimensions in Ref. [23].

In the following, we introduce the model and show some numerical calculations of quantities of interest such as the wave-front speed. To match reality, the model will be further extended to take into account inhomogeneities of the medium and diffusion of molecules. In Sec. VI, we discuss some possible biological interpretations of the general reaction scheme presented in Sec. III.

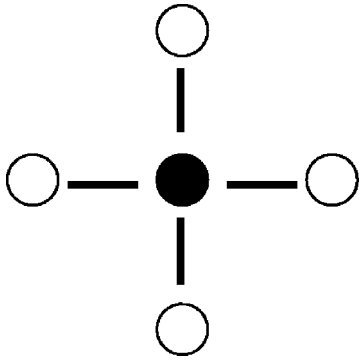

FIG. 1. Square lattice. An active particle represented by the black bullet in this figure may activate each of its four inactive neighbors.

III. THE MODEL REACTIONS

We model the intracellular space as a two-dimensional $L_1\times L_2=L$ lattice with $n=4$ nearest neighbors (Fig. 1). Each node of the lattice represents a molecule in one of three possible states: inactive (I), active (A), and refractory (R).

The boundary conditions of the lattice are periodic in the horizontal direction, whereas in the vertical direction we have open boundary conditions. The top row of the lattice represents the intracellular space in proximity of the cell membrane and the bottom row of the lattice represents either one of the following: (i) if L_2 is about the radius of a cell, then the last row represents the space limiting the nucleus membrane; in this case molecules cross the nucleus membrane or leave the signal to other mechanisms which would then take it inside the nucleus; (ii) if L_2 is much smaller than the radius of the cell, we represent a fraction of the cell and the activation of molecules beyond the last row of the lattice is neglected. In both cases, we investigate how the signal propagates from top to the bottom of the lattice (see Fig. 2).

Let $r(x,t)\in\{I,A,R\}$ be the state of node x at time t. Then we define $A(x,t)$ to indicate whether node x at time t is active or not [similarly we define $I(x,t)$ and $R(x,t)$],

$$A(x,t)=\begin{cases}1 & \text{if } r(x,t)=A\\ 0 & \text{otherwise.}\end{cases}$$

We start with the lattice filled with inactive molecules. This means that the medium is homogeneous [29]. At time $t=0$ one (or more) molecule in the first row of the automaton is flipped to the active state.

More formally, if we assign the left-lower corner of the lattice to the origin of the Euclidean plane and we set only the molecule in the middle point of the first row to the active state, then the initial setup can be written as follows: $\forall(x,y):x=0,\ldots,L_1-1,y=0,\ldots,L_2-1,(x,y)\neq(L_1/2,\ L_2-1)r((x,y),0)=I$ and $r((L_1/2,\ L_2-1),0)=A$.

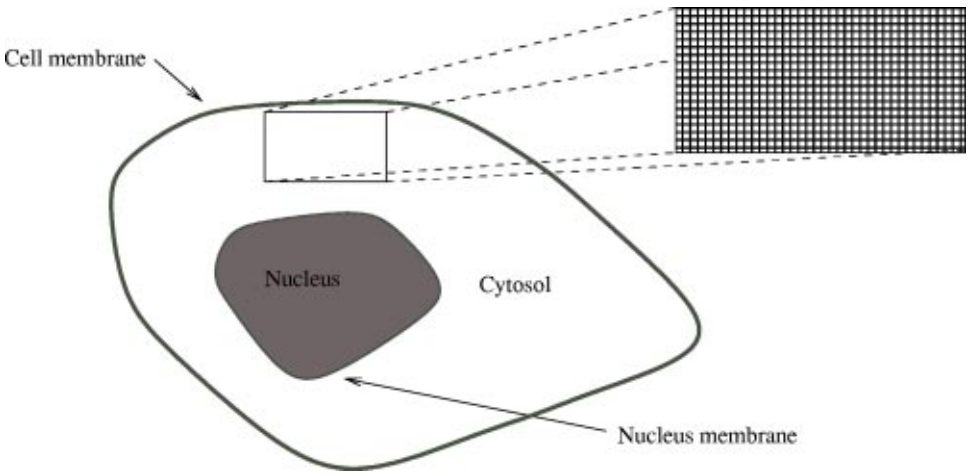

FIG. 2. Two-dimensional representation of the lattice as a limited region of the intracellular space in eukaryotic cells.

Each active site is able to catalyze any neighboring site. The reactions are the following:

$$A+I\rightarrow^{a} R+A, \tag{1}$$

$$A\rightarrow^{b} I, \tag{2}$$

$$R\rightarrow^{c} I,$$

where a, b, and c represent reaction rates as the probability that the reaction takes place. Note that the first reaction above is not ''local'' (it takes place among active molecules and inactive molecules belonging to nearest neighbors sites). Note also that in the case of no refractory state and $b\simeq 0$ and $c\simeq 0$, the reaction system reduces to $A+I\rightarrow 2A$ in two dimensions.

Because we allow up to $n=4$ reactions to take place in each neighbor of an active molecule (i.e., one active molecule may catalyze at most n inactive molecules) in one time step, we can recast Eq. (1) as follows:

$$A+kI\overset{\zeta(k)}{\rightarrow} R+kA, \tag{3}$$

where $k=0,1,\ldots,n$, and $\zeta(k)=\zeta_{a,n}(k)$ is the ''normalized'' reaction rate that takes into account the possibility of multiple (up to n) reactions in one time step. That is, $\zeta_{a,n}(k)$ is the probability density function of a binomial distribution with parameters a and n. A more precise formalism based on the Boolean functions $A(\cdot,\cdot)$,$I(\cdot,\cdot)$, and $R(\cdot,\cdot)$ is the following:

$$R(x,t+1)=A(x,t)\max_{i}\{I(x+\mathbf{c}_i,t)\omega_i(a,t)\},$$

$$A(x+\mathbf{c}_i,t+1)=A(x,t)I(x+\mathbf{c}_i,t)\omega_i(a,t),$$

$$I(x,t+1)=A(x,t)\omega(b,t)+R(x,t)\omega(c,t).$$

The right-hand sides give the conditions for the node x at time t, while the left-hand sides give the state at time $t+1$; $x+\mathbf{c}_i$ represents a neighbor of node x with $\mathbf{c}_i$, indicating the unit vector connecting a node to its nearest neighbor $i=1,\ldots,4$; $\omega_i(\cdot,t)$ is the ith independent realization of a Bernoullian event (i.e., a variable taking value 1 at time t with probability specified by the first argument).

Let

$$A(t)=\frac{1}{L}\sum_{x=1}^{L} A(x,t) \tag{4}$$

be the mean concentration of active molecules at time t. In the same way, we define $I(t)$ and $R(t)$ as the concentration of inactive and refractory molecules, respectively. Since each node of the lattice is found in one of three states, a consequence of Eq. (4) is a sum rule [24]:

$$A(t)+I(t)+R(t)=1 \quad \forall t.$$

Note that Eqs. (1) and (3) entail that the signal corresponding to the activated nodes of the lattice performs on average $0<a<1$ steps to one of the neighboring sites per unit time; an active node activates, with probability a, each of the inactive nodes in its neighbors. As a result there is no particle diffusion but propagation of the active state. This model is similar to the infection model studied in Ref. [25] where active means ''infected'' and the rule is that an infected particle may jump to a neighboring site and infect it with a certain probability.

A. Reference measures for simulated space and time

In this section we assess the physical values of the time step and lattice spacing used in the simulations. To distinguish physical quantities from simulated ones, we indicate the latter with the tilde (for example $\tilde{\Delta}t$).

The time step is defined according to the reaction time $\tilde{\tau}$. It can vary in the range 10^{-6}–1 s. This is quite a large range, which leaves us with great freedom in the choice of the parameters. In the present work, we take $\Delta t=10^{-3}$ s.

In our model each lattice point represents a molecule. The dimension of a molecule is about 10 nm and the diameter of a cell may vary from 20 μm to 1 mm. Thus we need

$$\frac{10\ \mu\text{m}-1\ \text{mm}}{10\ \text{nm}}=10^{3}-10^{5}$$

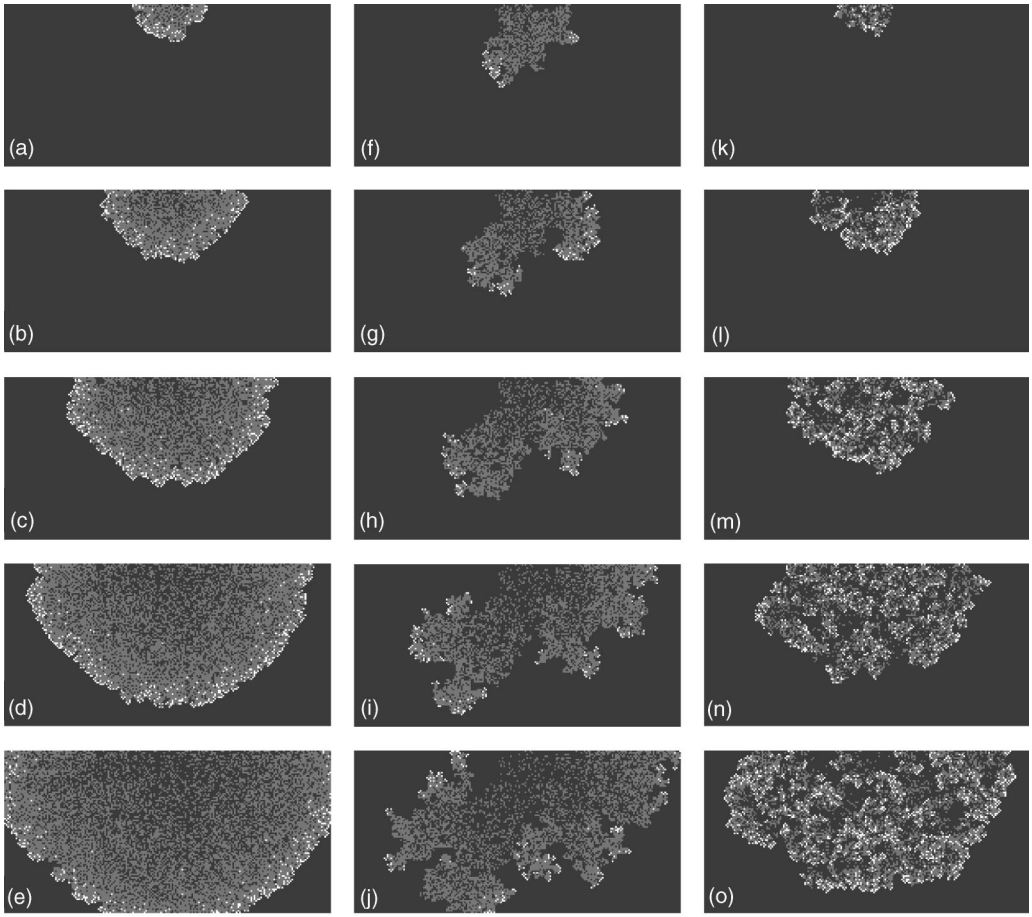

FIG. 3. A single node is activated at the top of the automaton. (a)–(e) are snapshots of a simulation with parameters $a=0.7$, $b=0.15$, $c=0.01$, and $L_1\times L_2=400\times 200$ (dark gray is I, light gray is R, and white is A). The evolution of a quite regular wave front is visible. (f)–(j) has same parameters as before but $b=0.25$. The wave front is much more irregular. (k)–(o) has same parameters but $b=0.25$ and $c=0.1$. No real wave front is recognizable and reactions take place everywhere within the space of propagation.

molecules. This means that in order to represent the distance between membrane and nucleus we need between 10^3 and 10^5 lattice points.

IV. KINETIC MONTE CARLO SIMULATIONS

The main parameters of the model are the size of the lattice and the reaction rates a, b, and c. The reaction rates determine the shape of the propagating wave and the duration of the activation of the medium, defined as the time taken by the system to relax to the initial inactive state.

In Fig. 3, we show five snapshots from three simulations with different reaction rates. It is possible to summarize the effects of the three parameters on the overall dynamics of the wave, as follows:

(i) The wave propagates down to the nucleus with a certain velocity which depends mainly on the reaction rate a.

(ii) The shape of the front is determined by the second parameter b. For small b the evolution of a quite regular wave front is visible [see Figs. 3(a)–3(e)] whereas for larger b the front is more irregular [Figs. 3(f)–3(j)].

(iii) The value of c controls the capability of relaxation to the original state [note the presence of much higher activity in Figs. 3(k)–3(o)]. Reactions take place everywhere within the space of propagation.

This last observation deserves further discussion. The wave-based mechanism requires relaxation of the medium once the wave has reached the target nucleus. The relaxation to the initial condition is a general characteristic of many biological systems. In the specific case of signal transduction it sets the requirement for the cell to go back to the original state, ready to respond to subsequent signals.

In Fig. 4, we show the effect of the reaction rate c on the overall dynamics of the active molecular concentration $A(t)$. In two of three runs the system does not relax to the initial condition. In particular, for $c>0.005$ biologically unrealistic oscillatory behavior is found. We define some quantities that will be useful in the following. Call $\hat{t}$ the time at which the first active molecule reaches the last row of the lattice

$$\hat{t}=\min_t\{\exists x_{\hat{t}}=0,\ldots,L_1-1,\ A((x_{\hat{t}},0),t)=1\}.$$

Also, define the displacement from $L_1/2$,

$$d=\left|x_{\hat{t}}-\frac{L_1}{2}\right|.$$

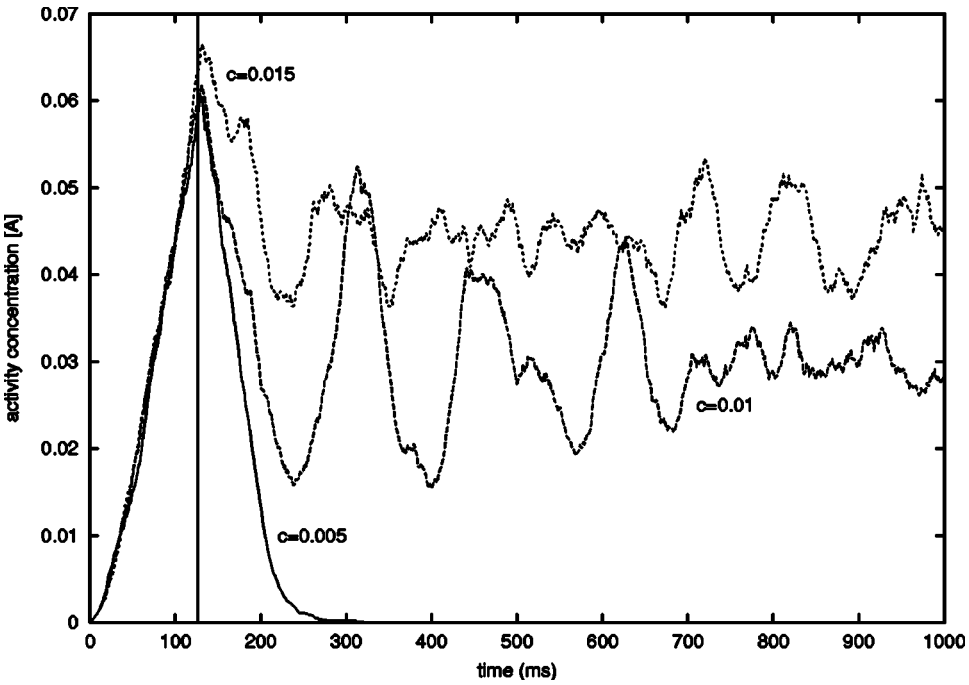

FIG. 4. Effect of the reaction rate c on the overall dynamics of the concentration of the active molecules. Parameters: $a=0.7$, $b=0.05$, and $L=200\times100$. The vertical line roughly indicates the moment in which the signal reaches the nucleus. In two of these runs the system does not relax to the initial condition. As a result, apart from fluctuations, these two parameter setups cannot be given any biological relevance.

The front velocity is then defined as

$$v=\|\vec{v}\|=\frac{\sqrt{L_2^2+d^2}}{\hat{t}}. \tag{5}$$

Following Sec. III A, this is expressed in nm/ms. Moreover, we define

$$\theta=\frac{\arctan(d/L_2)}{\pi/4},$$

which is the angle between the vertical axis and the line traced between the points (x_0,L_1-1) and $(x_{\hat{t}},0)$, normalized to 1 (recall that $L_2=L_1/2$). The angle θ is a raw indicator of the defocusing.

We have performed a set of 50 independent runs for each value of the three parameters a, b, and c and calculated the wave velocity according to Eq. (5). The results are shown in Figs. 5–7, respectively. Each figure shows v versus a,b, and c for a fixed setup of the lattice size L. Points are the average computed over the 50 measurements and error bars represent the standard deviation. The inset plot of each figure shows θ versus the parameter value.

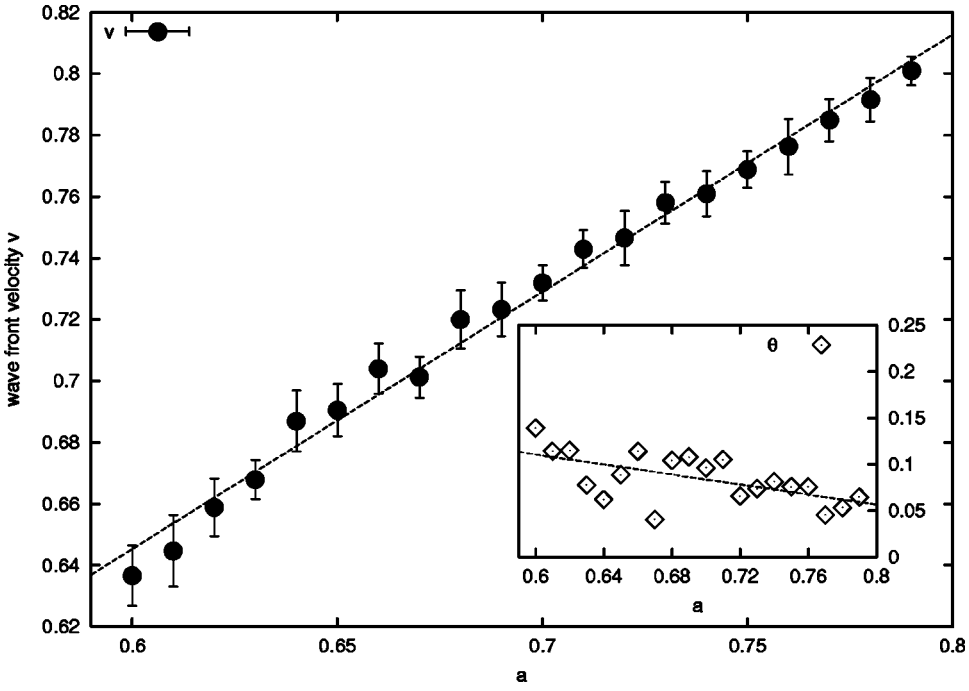

FIG. 5. Wave-front velocity v (in units of nm/ms) versus a. Each point is calculated averaging the velocity over 50 independent realizations (error bars indicate deviation from the mean). Parameters: $L=1000\times500$, 1000 time steps, $b=0.15$, and $c=0.01$. Slope of the linear fit is 0.837. $\theta(a)$ shown in the inbox as function of a, and slope of the fit is -0.22.

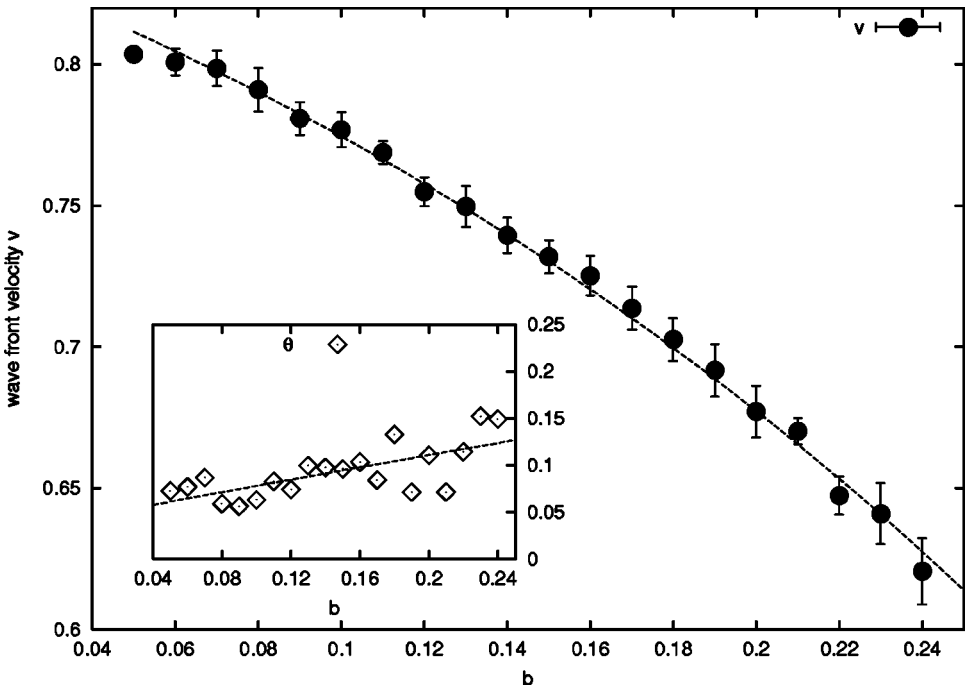

FIG. 6. Wave-front velocity v (in units of nm/ms) versus b. Parameters: $a=0.7$, $c=0.01$. Same lattice size and time steps as in Fig. 5. Points are fitted with the function $1-\alpha_1\exp(\alpha_2 x)$, with $\alpha_1=0.158$, $\alpha_2=3.584$. $\theta(b)$ in the inbox, slope 0.26.

As mentioned earlier, the front velocity v depends linearly on the reaction rate of the forward reaction a. It is worth noting in Fig. 5 that the standard deviation decreases with increasing a indicating a correlation between a and the smoothness of the front propagation. In fact, the inset plot in the same figure shows θ as a function of a. A linear fit gives a slope equal to -0.22 indicating a linear focusing effect.

The effect of varying b is shown in Fig. 6. Here the correlation with the velocity is negative. This is explained by the fact that for high b the front is much more indented, thus reducing the speed. Indeed the effect of larger values for the inactivation reaction rate b is visible in Fig. 3(c).

Note that both Figs. 5 and 6 show that the front speed v is maximal when θ is minimal. Thus we may write $v\propto 1/\theta$, in qualitative agreement with Ref. [20].

Changes in the rate c do not produce visible effects on the velocity. In fact, Fig. 7 shows no significant dependence of v on c. What is affected by c is the asymptotic behavior of the activity concentration $A(t)$, as already shown in Fig. 4. In other words, the rate c for the reactivation of the inactive state plays no role in determining the front velocity, whereas it determines the duration of the overall activation time. For values of c above a certain threshold (which in turn depends on a and b) the reaction never ends, following an oscillatory

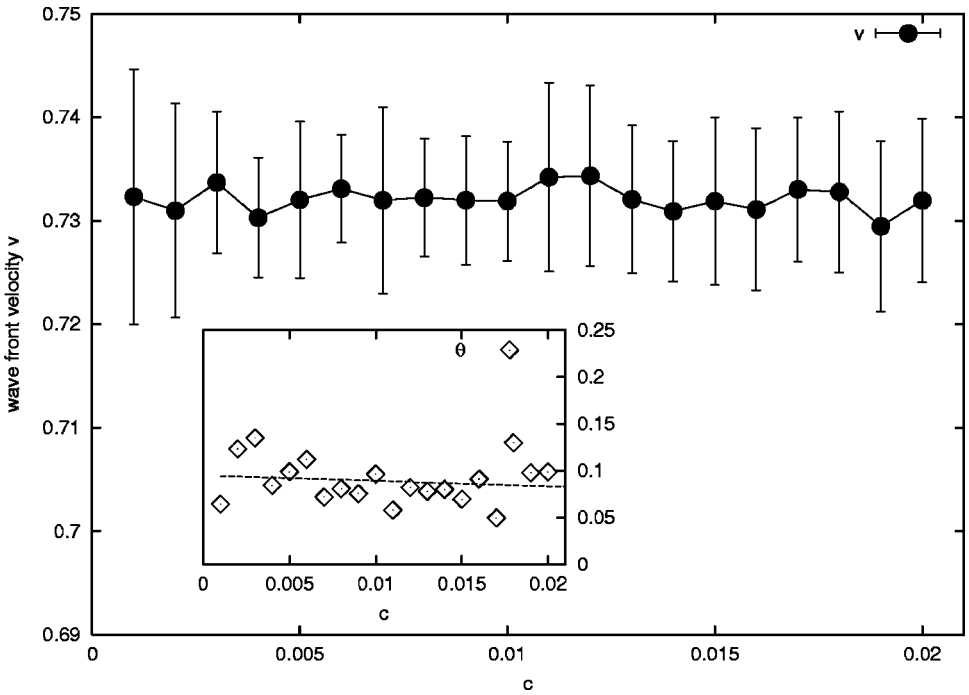

FIG. 7. Wave-front velocity v (in units of nm/ms) versus c. Parameters $a=0.7$, $b=0.15$. Remaining parameters as in Figs. 5 and 6. In the inbox the fit's slope is -0.45.

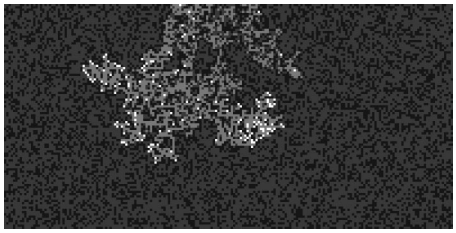

FIG. 8. The effect of propagating the signal in a porous medium ($p=0.65$). Black is *O*, dark gray is *I*, light gray is *R*, and white is *A*.

asymptotic behavior. The asymptotic level of activity is inversely proportional to c, which is quite intuitive given that $1/c$ is the time the particle or molecule remains in the refractory state.

All the numerical data produced by these simulations indicate that to have a relaxation to the initial condition of the medium, the reversing rates b and c must be much smaller than the forward reaction rate a.

V. FURTHER EXTENSIONS AND SIMULATIONS

For the cytoplasm, the basic assumption of homogeneity in the previous model is clearly too strong an approximation. Also, in the cytoplasm, molecules are free to diffuse.

A. Percolation in a porous medium

To take into account such inhomogeneities, we treat the cytosol as a porous medium. However, we are forced to neglect organelles, which are orders of magnitude bigger than molecules. This leads to consider spurious elements other than the molecule carrying the signal. We identify those spurious molecules labeling a node with *O*.

Initially, the lattice is filled as before with molecules in the inactive state but this time we put a molecule in a node with probability $p \neq 0$ whereas, with probability $1-p$, we fill it with *O* (Fig. 8).

As a result, $r(x,t) \in \{I,A,R,O\}$.

From the geometrical and physical viewpoint this is a typical percolation lattice. So we could expect that at a certain critical value p_c (called the *percolation threshold*, which depends on the lattice topology and dimension), the probability to have a single cluster of neighbor nodes spanning the whole lattice (called the infinite cluster) is close to 1 [26].

Actually, in our setup, the existence of a percolating cluster does not necessarily imply that signal reaches the nucleus since this depends also on the chemical dynamics of the autocatalytic reactions, which in turn depends on the value of the specific chemical parameters.

The parameter p can be identified as a measure of the density of the medium. In the following section, we study the way such density affects the propagation of the signal.

1. Simulations

We have performed a set of 50 simulations for different values of p and computed the velocity v as the average of the different outcomes. Figure 9 shows v versus p for a fixed

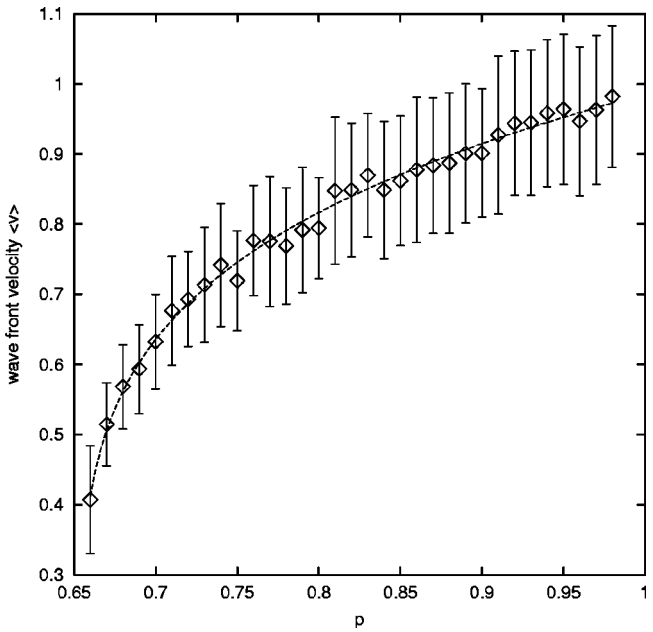

FIG. 9. Wave-front velocity v (expressed in nm/ms) as function of p is plotted for the parameter's setup $a=0.75$, $b=0.05$, and $c=0.01$. Velocity is computed averaging on 50 independent runs (error bars show the standard deviation). Dashed line represents the best fit with the hyperbolic function $x^{1/\beta}$ with exponent $\beta=4.76$.

choice of a, b, and c. As expected v grows with p. The best fit of the numeric data is found with the hyperbolic function $p^{0.21}$.

Figure 10 shows the relation of the velocity v with respect to both a and b. It appears that for increasing values of p the effect of a larger forward reaction rate a is stronger than the damping effect of the reverse reaction rate b. Note that for a given p, only a limited set of choices of a, b, and c guarantees that the system relaxes to the quiescent state once the signal has reached the nucleus. However, as previously shown, the parameter c does not influence the value of the velocity v. Also note that $v=0$ in Fig. 10, at variance with standard percolation problems, indicates either that no infinite cluster exists or that the signal expires before reaching the nucleus depending on the values of the parameters. This suggests that the activation of the cell may follow an *all-or-none* rule, which depends critically on the concentration of the extracellular hormones that induce the signal. To test such a conjecture, we performed similar (numerical) experiments to those reported in Ref. [27]. There, a thresholdlike effect is observed in *Xenopus oocytes* maturation-inducing hormone progesterone. One of the results on the MAPK (mitogen-activated protein kinase) cascade transduction, is that the concentration of extracellular hormone induces oocyte maturation only above a certain threshold.

We find similar results in our simulations. They are shown in Fig. 11. The activation level in the y axis is defined as the ratio of successful runs over a sample of 50, that is the number of runs for which the signal reaches the nucleus. This level is plotted against the hormone concentration, defined as the number of active lattice nodes on the first row, divided by L_1. Data has been fitted with a Hill function, as in Ref. [27].

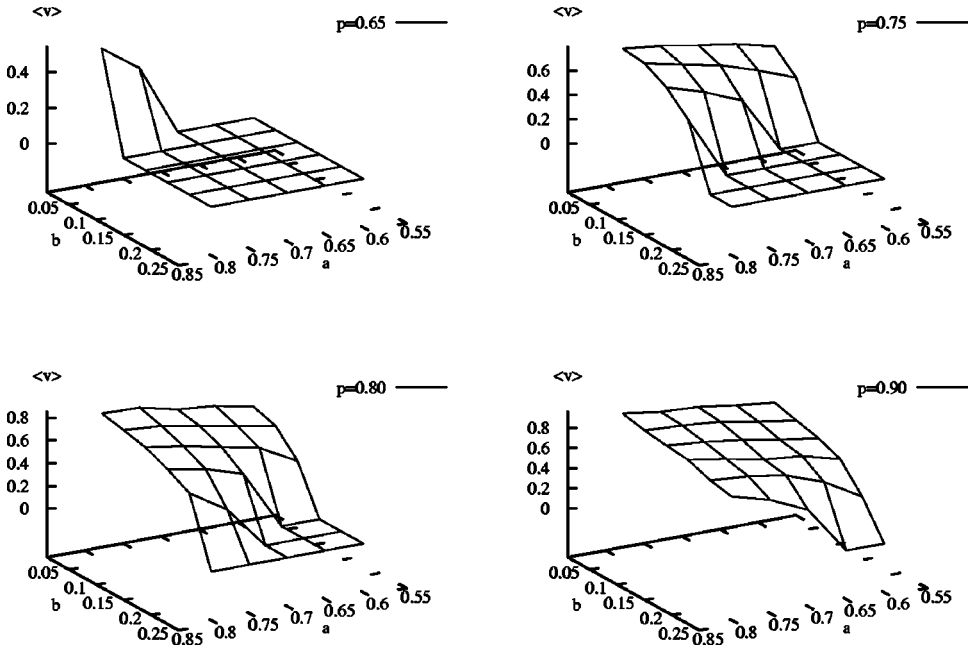

FIG. 10. Wave-front velocity v (units of nm/ms) as function of a and b for four values of p. Velocity is computed averaging on 50 independent runs, c has been fixed to 0.01.

The Hill function is defined as follows:

$$H_m(x) = \frac{x^m}{C^m + x^m},$$

where m is the Hill coefficient and C is a constant. The Hill coefficients of the fits for the data shown in Fig. 11 are reported in Table I. The parameter C, which determines the ''critical'' concentration, decreases with increasing p, whereas the Hill coefficient m, which corresponds to a sharper transition, shows a nonmonotonic relationship with p.

B. Effects of slow diffusion of molecules

A wider class of phenomena can be described by including the diffusion of particles or molecules, for instance the propagation of a wave into an unstable medium, as reported in Ref. [28]. The metastable case (for which the stable case $p=0$, $D=0$ is a special case) is simpler and better understood then the unstable case. Basically, when particles or molecules may diffuse, active particles act as sources of new waves. Thus, the front propagation is the result of the interference of many propagating wave fronts [30]. Indeed if the wave front in the two-dimensional lattice breaks down, many fronts propagating in all directions arise in a short time. At each time step, new fronts are generated by the reshuffling of the position of the active particles that constituted a single bigger front at the previous time step. Since diffusion does not have a preferential direction, each diffusion step breaks down the fronts into smaller frontlets propagating in all directions.

Although the reshuffling of the wave front transforms the signal propagation into a random walklike diffusion, the general conclusion is that a necessary condition for the existence of a coherent signal (that is an impulse) is that the refractory state needs to last long enough. It is not difficult to understand that if such condition is not met, then the reaction may result in a never ending chain reaction.

Figure 12 shows the activation level versus hormone concentration with and without slow diffusion. In the diffusive case, molecules jump to *empty* neighbors (if any) with probability 10^{-1} and $p=0.662$. As expected, the signal propagates more efficiently as compared to the nondiffusive case.

VI. DISCUSSION

As we have seen, the density affects the smoothness of the wave front determining, in the case of high density, a clear

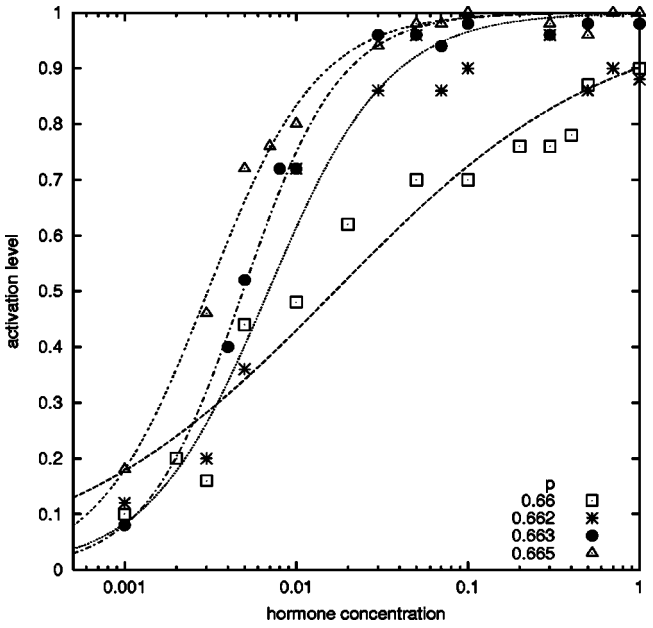

FIG. 11. Stimulated cells versus hormone concentration. Parameters: $a=0.75$, $b=0.05$, $c=0.01$, and $L_1=1000$. Hill coefficients of the fitting curves in Table I.

TABLE I. Hill coefficients for different values of p relative to the data shown in Fig. 11.

p	m	C
0.660	0.598	0.019
0.662	1.610	0.009
0.663	1.283	0.005
0.665	1.358	0.003

front wave, thus a higher propagation velocity. As a matter of fact, the cytoplasm, though dense, is not homogeneous and areas of low density are interlaced with areas at high density. As a result, the propagation assumes the connotation of a wave in high-density domains, whereas in low-density regions molecules fluctuate randomly without a preferred direction.

A solid assessment of such theoretical scenario should proceed through the search for plausible biochemical reactions in pathways. A possible candidate for the ''forward'' reaction (1) could be the *phosphorylation*, with the active state represented by an activated (phosphorylated) *kineses*, whereas inactive means the unphosphorylated reactant. On the other hand, the ''backward'' reaction (2) would represent dephosphorylation of phosphorylated reactant, which implies the existence of the corresponding phosphatase [31].

The main problem with this biochemical representation is the existence of the refractory or exhaust state. This corresponds to the situation in which there is no ready-to-be-phosphorylated molecule in the close vicinity in *short time*. Two possible candidates are given below.

(i) The first takes into account the activation of an inhibitor of the reaction. This may be achieved if the catalyzer of the main reaction (the autophosphorylation) is also a catalyzer of a reaction producing phosphatases.

(ii) In a chemical phosphorylation reaction, the ''fuel'' is represented by the *adenyn triphosphate molecule* (ATP for short). In general, in the cell, ATP is present in a very large quantity. Indeed it is continuously used for a number of different reactions and it is produced at a very fast rate by the processing of the glucose molecules. Nevertheless, the local concentration of ATP drops as a consequence of high phosphorylation local rate, and some time (though short) is required for the local concentration to return to previous value thanks to metabolic ATP replenishment and diffusion.

VII. CONCLUSIONS

We have studied a simple reaction scheme in a two-dimensional lattice of particles or molecules with a refractory state.

Our major goal was to show that the phenomenon of signal transduction in a cell can be explained as a chemical wave of activation of molecules in the cytosol. In particular, we have shown that a sufficient condition for the onset of a wave of activation toward the nucleus is the existence of at least one autocatalytic reaction in the chain of reactions constituting the cascade.

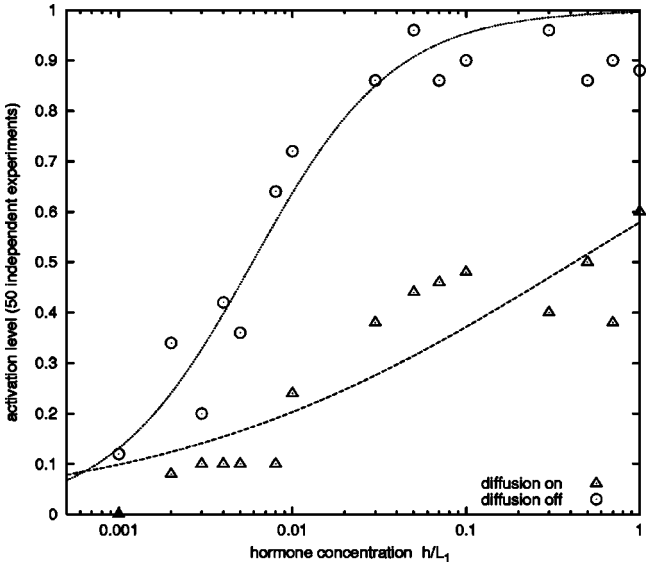

FIG. 12. Activation level versus hormone concentration with and without slow diffusion of molecules into empty nodes of the lattice for $p=0.662$. Diffusion is such that a molecule takes, on average, 10 time steps to move between two neighboring sites.

Numerical studies of the more complex case of inhomogeneous medium and slow diffusion of the molecules suggest that the signal propagates as a wave in areas of high concentration of metabolites, whereas in low-density regions of the cytoplasm the propagation is mainly carried by random diffusion. Such combined mechanism allows the signal to propagate on a longer distance in a shorter time as compared to a bare random walk. This could explain the relative fast responses observed experimentally in ''large'' cells such as eggs.

This point deserves further investigation and, possibly, experimental confirmation.

ACKNOWLEDGMENTS

This work has been performed during the stay of F. Castiglione at the Department of Cell Biology of the Harvard Medical School, Boston. F. Castiglione, M. Bernaschi, and S. Succi wish to thank the Giovanni Armenise—Harvard Foundation for financial support. Fruitful discussion with T. Höfer and R. King are kindly acknowledged. F. Castiglione also thanks the Center for Applied Computer Science (ZPR/ZAIK) of the University of Cologne, for computing time.

[1] L.H. Hartwell, J.J. Hopfield, S. Leibler, and A.W. Murray, Nature (London) **402**, C47 (1999).
[2] D. Endy and R. Brent, Nature (London) **409**, 391 (2001).
[3] W.W. Gibbs, Sci. Am. August (2001), p. 53.
[4] J.H. Lodish, A. Berk, S.L. Zipurky, P. Matsudaira, D. Baltimore, and J. E. Darnell, *Molecular Cell Biology*, 4th ed. (W.H. Freeman and Company, New York, 2000).
[5] M.J. Robinson and M.H. Cobb, Curr. Opin. Cell Biol. **9**, 180

(1997).
[6] A. Salic, E. Lee, L. Mayer, and M.W. Kirschner, Mol. Cell **5**, 523 (2000).
[7] R. Heinrich (unpublished).
[8] P. Polakis, Genes Dev. **14**, 1837 (2000).
[9] M.J. Seidensticker and J. Behrens, Biochim. Biophys. Acta **1495**, 168 (2000).
[10] T. Höfer, A. Politi, and R. Heinrich, Biophys. J. **80**, 75 (2001).
[11] I. Aranson, H. Levine, and L. Tsimring, Phys. Rev. Lett. **76**, 1170 (1996).
[12] H. Levine, I. Aranson, L. Tsimring, and T.V. Truong, Proc. Natl. Acad. Sci. U.S.A. **93**, 6382 (1996).
[13] K.W. Lee, S.E. Webb, and A.L. Miller, Dev. Biol. **214**, 168 (1999).
[14] P. Gray and S.K. Scott, *Chemical Oscillation and Instabilities* (Clarendon Press, Oxford, 1990).
[15] R.A. Fisher, Proc. Annu. Eugen. **7**, 353 (1937).
[16] A. Kolmogoroff, I. Petrovsky, and N. Piscounoff, Moscow Univ. Bull. Math. **1**, 1 (1937).
[17] B.P. Belousov, in *Oscillations and Travelling Waves in Chemical Systems*, edited by R. J. Field and M. Burgher (Wiley, New York, 1985), pp. 605–613.
[18] A.M. Zhabotinskii, Biofizika **9**, 306 (1964).
[19] A.M. Zhabotinskii and A.N. Zaikin, Nature (London) **225**, 535 (1970).
[20] M. Gerhardt, H. Schuster, and J.J. Tyson, Science **247**, 1563 (1990).
[21] J.R. Weimar, J.J. Tyson, and L.T. Watson, Physica D **55**, 309 (1992).
[22] J. Mai, I.M. Sokolov, and A. Blumen, Phys. Rev. E **64**, 011102 (2001).
[23] J. Mai, I.M. Sokolov, and A. Blumen, Phys. Rev. E **62**, 141 (2000).
[24] J.P. Boon, D. Dab, R.K. Kapral, and A. Lawniczak, Phys. Rep. **273**, 55 (1996).
[25] J. Mai, I.M. Sokolov, and A. Blumen, Phys. Rev. Lett. **77**, 4462 (1996).
[26] D. Stauffer and A. Aharony, *Introduction to Percolation Theory*, 2nd ed. (Taylor and Francis, London, 1994).
[27] J.E. Ferrell, Jr., and E.M. Machleder, Science **280**, 895 (1998).
[28] D.A. Kessler, Z. Ner, and L.M. Sander, Phys. Rev. E **58**, 107 (1998).
[29] In Sec. V A empty nodes in the lattice will be introduced to model inhomogeneity in the medium.
[30] Note that in our model this may also happen even in the stable-medium case ($p=0$, $D=0$) if appropriate values for the parameters are chosen [see Figs. 3(k)–3(o)].
[31] Phosphorylation is a chemical reaction involving a reactant and one element of the phosphate group called kinase. The reaction consists of transferring a phosphate group from an adhenyntriphosphate (ATP) to the reactant. Dephosphorylation is the reverse process of phosphorylation and uses phosphatase as enzyme. A phosphorylated substrate is brought into the unphosphorylated state by means of the phosphatase enzyme [4].